

# An Integrated Continuous Class- $F^{-1}$ Mode Power Amplifier Design Approach for Microwave Enhanced Portable Diagnostic Applications

Azeem Imtiaz, *Member, IEEE*, Jonathan Lees, Heungjae Choi, *Member, IEEE*, and Lovleen Tina Joshi

**Abstract**—This paper presents a novel technique for designing a microwave power delivery system targeted at compact and portable microwave-assisted diagnostic healthcare applications to help tackle the growing problem of anti-microbial resistance. The arrangement comprises a purpose-built cylindrical cavity resonator within which, the bacterial samples are exposed, driven by a high-efficiency 10-W GaN amplifier, critically coupled via a simple, adjustable internal loop antenna. The experimental work considers the exposure of different sample volumes of water and the change in the natural impedance environment of the cavity that results. For the first time, it is shown that impedance variation cannot only be accommodated, but can actually be exploited, allowing “continuous,” high-efficiency performance to be achieved while processing a wide range of sample volumes. Specifically, using only transistor package parasitics, the impedance of the cavity itself together with a single-series transmission line allows a continuous class- $F^{-1}$  mode loading condition to be realized. Measured results show more than 70% average drain efficiency, above 40-dBm average output power, and more than 10-dB gain over the cavity’s operational bandwidth.

**Index Terms**—Anti-microbial resistance (AMR), bacterial spore, *C-difficile*, class- $F^{-1}$ , continuous modes, DNA detection, GaN, healthcare, microwave heating, power amplifier (PA).

## I. INTRODUCTION

SINGLE-MODE microwave resonant cavities driven by high-efficiency microwave power amplifiers (PAs) are enabling many applications within research, industry, and healthcare-related fields. Examples of these include polymer curing for the production of microcapsules for drug delivery, curing large-scale components for the aerospace industry, as well as the assisted curing of new types of environmentally friendly concrete. Developing research is also looking at tumor ablation, bacterial biofilm disruption, water sterilization, additive manufacture monitoring, hydrogen storage, heavy-oil cracking, and others. Most of these applications have the

potential for commercialization (and hence integration), and all use resonant cavity structures capable of allowing almost all (typically  $> 99\%$ ) of the generated microwave power to be delivered into a sample or device. Each of these cavities typically needs to be driven by a high-efficiency microwave amplifier developing power between 1 and 300 W, and, due to the load-dependent resonant properties, these microwave power generators need to be frequency-agile and able to operate over wide bandwidths.

In terms of healthcare applications, the spread of anti-microbial resistance (AMR) is a growing threat to our ability to treat infectious disease, due largely to the “blind” prescribing of antibiotics. This is, in part, a consequence of our inability to determine the antibiotic susceptibility of infecting bacteria sufficiently rapidly in *real time*. Current bacterial detection methods take at best several hours to produce results and tend to be used to confirm rather than to prevent infection.

In this paper, it is described how high-efficiency microwave amplifiers and microwave resonant cavities are enabling a prototype bacterial DNA detection system that is able to confirm presence of specific pathogens within minutes instead of hours; this is a significant change that has the potential to reduce patient suffering and morbidity and help extend the utility of the remaining effective antibiotics.

Although using microwave techniques for disruption and sensing in medical and healthcare applications offers many advantages, previous work in this field has been limited to using conventional microwave ovens and metallic bow-tie structures deposited on glass. Due to the use of magnetrons and multimode cavities, this apparatus proved unreliable, inefficient, physically large, imprecise, with difficult to control and required mains level voltage to operate.

In the microwave-enhanced diagnostic application targeted in this work, high microwave field within a circular cavity resonator is used to disrupt not only bacterial vegetative cells but also spore, such that bacterial DNA can be easily detected using patented, rapid, high-sensitivity, and high-selectivity biochemical assays. For this bedside, portable, and potentially field-deployable apparatus, compactness, high power efficiency, frequency agility, ease of integration, and measurement accuracy are all critical aspects of the design.

Solid-state microwave generation for diagnostic and sensing systems has, over the years, attracted the attention of medical and engineering professionals alike. For example, beam-focused annular arrays of microstrip patch antennas studied in

Manuscript received April 01, 2015; revised June 08, 2015; accepted August 19, 2015. Date of publication September 16, 2015; date of current version October 02, 2015. This work was supported by NXP Semiconductor, Nijmegen, The Netherlands, under Cardiff University’s Presidents Scholarship scheme.

A. Imtiaz, J. Lees, and H. Choi are with the School of Engineering, Cardiff University, Cardiff, CF 24 3AA, U.K. (e-mail: azeem.imtiaz@gmail.com; leesj2@cardiff.ac.uk, choih1@cardiff.ac.uk).

L. T. Joshi is with the School of Pharmacy, Cardiff University, Cardiff, CF 24 3AA, U.K. (e-mail: joshilt@cardiff.ac.uk).

Color versions of one or more of the figures in this paper are available online at <http://ieeexplore.ieee.org>.

Digital Object Identifier 10.1109/TMTT.2015.2472417

[1]–[3] are currently in use for noninvasive treatment of tumors in the head, neck, and pelvic region of the human body.

More recently, and associated with this work, rapid detection ( $\leq 4$  min) of *C-difficile*, anthrax, and tuberculosis using advanced biochemical DNA detection techniques have been patented in [4]. Similarly, in [5] and [6], a fully integrated solid-state microwave heating system is demonstrated in which a cavity resonator is directly presented to the LDMOS power transistor. The work presented in this paper significantly expands previous work in two aspects.

First, through the novel application of continuous-mode theory, this apparatus has the ability to accommodate the load impedance variations that result from treating different volumes of water samples, while working over the operational bandwidth of the cavity—which is a scenario that would typically exist in the targeted application

Second, it formulates the continuous class- $F^{-1}$  power amplifier mode by utilizing the built-in package network of the 10-W GaN transistor, together with simple series transmission lines. Using these techniques, a high-efficiency continuous  $F^{-1}$  PA has been designed using a dramatically simplified matching network.

Continuous-mode amplifier design is a relatively new concept, and the “normal” application space is transmitter design for wireless communication systems. The approach is attractive in that it is able to tolerate and even exploit the varying impedances presented by a fixed matching network and deliver consistently high power and efficiency over wide or very wide operational bandwidths. This biomedical application is different in that the load is not a matched load or antenna, but is a single-mode resonant cavity containing a biological sample, with significant fundamental and harmonic impedance change caused by variations in key sample parameters including volume, consistency, and temperature. The impedance variation at the fundamental frequency for example manifests itself as a shift in the cavity's resonant frequency, which can change significantly with variation in these parameters.

It is important to stress that, to ensure high ( $> 90\%$ ) efficiency in terms of delivering generated radio-frequency (RF) power into the cavity, the frequency of excitation needs to change in response to the resonant frequency of the cavity, minimizing the reflection coefficient.

This technique significantly reduces the complexity and physical size of matching networks typically required for broadband amplifiers. For example, the conventional broadband class- $F^{-1}$  PA presented in [7] used a complicated and physically large output matching network together with the built-in transistor package network. The comparison of both “conventional” and compact continuous class- $F^{-1}$  design approaches is shown in Fig. 1 (note that two different device types are used here with different parasitic networks).

Achieving high power delivery and good power efficiency when driving a resonant cavity is problematic because of the sensitivity of the resonant mode to any perturbations of the load. In other words, it is difficult to control the fundamental and harmonic load impedance environment presented by the cavity as it changes significantly when the volume, temperature, and consistency of the sample is varied, as would likely be the case in a

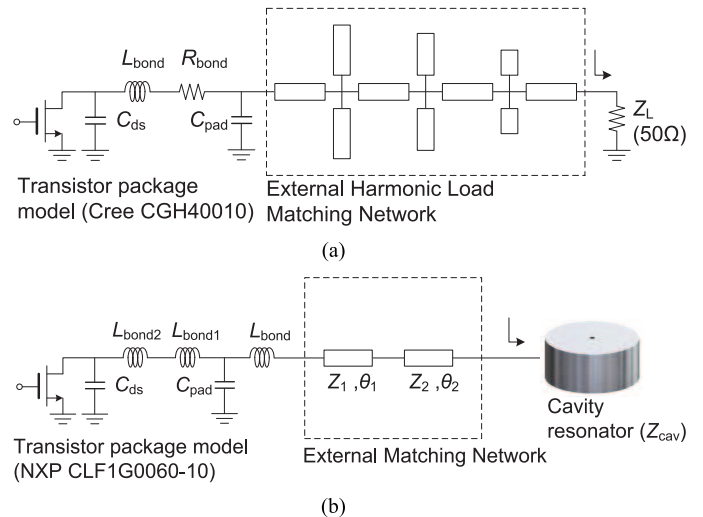


Fig. 1. Matching circuit design incorporating package parasitic components for (a) conventional 50- $\Omega$  continuous class- $F^{-1}$  design using a CREE 10-W GaN (CGH4001010) power transistor [7]. (b) Simplified, compact direct match design, again incorporating package parasitics, using a similar NXP 10-W GaN device (CLF1G0060-10).

practical healthcare setting. This is compounded by the fact that, in the optimized, adaptive system envisaged, the frequency of the excitation would need to be precisely adjusted to accommodate shifts in resonant frequency. However, in this work, it is shown that the efficiency of a microwave heating system can be increased by designing a broadband matching network that can accommodate changes in the impedance environment of the cavity resonator due to such variations, through the adoption of continuous-mode PA matching techniques [7].

A broadband class- $F^{-1}$  matching network, consisting of a transistor package network together with series microstrip lines has been designed to accommodate the volume dependent changes in the impedance environment of the circular cavity. The integrated matching network ensures the reflection coefficient of the cavity at the intrinsic plane of the 10-W GaN transistor and allows continuous mode operation to be achieved. The precise relative phasing of the fundamental and second-harmonic loads at the current generator plane ( $I_{GEN}$ -plane) allows a high RF performance to be maintained over the functional bandwidth of the cavity resonator.

Unlike “conventional” 50- $\Omega$  continuous class- $F^{-1}$  PA design approaches [7], [8], this method relies on a “direct integration” approach and eliminates the need for the additional and physically large harmonic tuning networks connecting the PA to the resonator, together with their associated loss. Further, integration has been considered by introducing a directional coupler into the output stage of the PA in order to monitor the delivered and reflected power to enable some degree of performance analysis as well as to ultimately provide a means of adaptive control.

## II. INTEGRATED DESIGN METHODOLOGY

Characterization of the critically coupled cavity while varying water volume and then importing the combined, volume-dependent one-port  $S$ -parameter file into a nonlinear circuit simulator allowed the loaded cavity to be dynamically modeled. In summary, the design process has been divided into

two stages, the first involving the characterization of the resonator under dynamic loading conditions (variation in sample volume) and the second focusing on multiharmonic load-pull characterization of the transistor. These stages are summarized in more detail below.

First, it was important to capture, in detail, the critically coupled impedance environment of the cavity by varying the volume of the sample (water) between 100 to 300  $\mu\text{L}$  in 20- $\mu\text{L}$  steps. Following this, a 10-W GaN high-electron mobility transistor (HEMT) power transistor was characterized using a multiharmonic active load-pull measurement system [15], in order to identify optimum performance parameters and a class-F<sup>-1</sup> mode of operation, which was later extendable to the required continuous class-F<sup>-1</sup> mode.

Once the intrinsic and package-plane optimum harmonic impedances had been identified, it was possible to design a simplified broadband class-F<sup>-1</sup> matching network to transform the measured cavity impedance environment to the required continuous mode impedances for presentation to the intrinsic output plane of the 10-W GaN transistor. This was done firstly for class-F<sup>-1</sup>, and later extended to continuous class-F<sup>-1</sup>. A simple directional coupler was embedded at the output stage of the amplifier to measure the system performance for different water volumes, allowing the complete structure to be measured and evaluated.

#### A. Measurements of the TM<sub>010</sub>-Mode Circular Cavity

Commercial microwave ovens comprise large, multimode resonant cavities excited by a relatively broadband (20-MHz) microwave source (magnetron). Although highly effective for domestic cooking and a wide variety of industrial applications, the complex impedance environment and unpredictable field distribution within these cavities restrict their use for precision microwave heating and disruption purposes where the controlled delivery and dosage is critical. In contrast, single-mode cavity resonators having well-defined impedance environments, well-defined resonant modes, and uniform and predictable electric ( $E$ ) and magnetic ( $H$ ) field distribution offer many possibilities in both industry and academia [9], [10]. In this experimental work, a TM<sub>010</sub>-mode, loop-coupled circular cavity resonator was designed to operate at a resonant frequency of 2.5 GHz.

The cross-sectional views of both halves of this cavity are shown in Fig. 2(a), and the  $E$ -field distribution (unloaded and 300- $\mu\text{L}$  water loaded) is shown in Fig. 2(b). The cavity was initially loaded with a plastic Eppendorf tube containing 300  $\mu\text{L}$  of water ( $\epsilon_r = 74$ ). Critical coupling into the  $H$ -field was achieved by careful adjustment of the position and orientation of the coupling loop in Fig. 2(a). Once critically coupled to a nominal volume, the first  $S$ -parameter measurement was taken, and minimum  $S_{11}$  was found to be  $-23$  dB, as shown in Fig. 3.

The water volume was then reduced in 20- $\mu\text{L}$  steps from 280 to 100  $\mu\text{L}$ , at which point, for a fixed coupling position, the cavity became excessively reflective (insertion loss  $> 3$  dB). This experiment resulted in ten discrete  $S_{1P}$  data files with each file containing the one-port  $S$ -parameters of the cavity corresponding to a specific water volume.

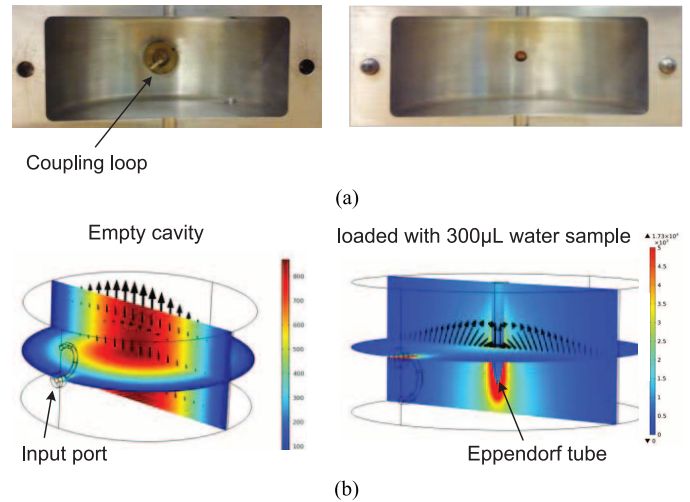


Fig. 2. (a) TM<sub>010</sub> circular cavity showing both hemispheres as well as the coupling loop. (b)  $E$ -field distribution (V/m)—simulated using COMSOL multiphysics package at 2.5 GHz.

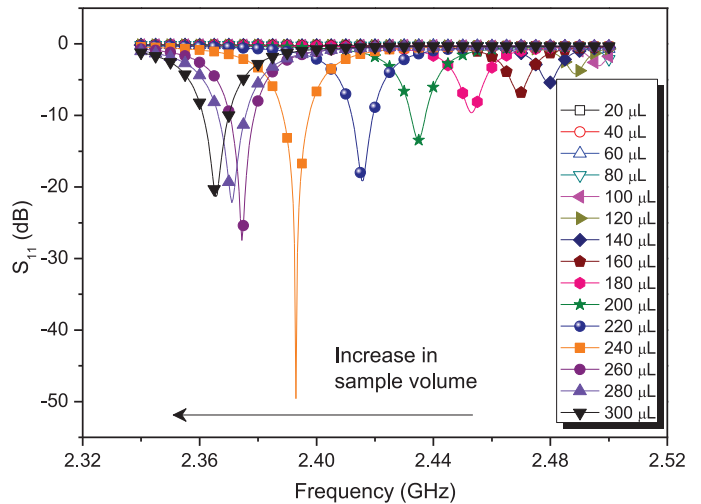


Fig. 3. Measured TM<sub>010</sub>-mode circular cavity response showing resonant shift due to varying water volume.

To utilize the measured cavity response offline in a computer-aided design (CAD) software, the files were combined into single multidimensional interchange format (MDIF) file and imported into the nonlinear circuit simulator (Advanced Design System (ADS), Keysight Technologies) for the next stage of the process—the PA design. The natural change in the fundamental and harmonic band impedance environment of the circular cavity as a function of water volume can be observed in Fig. 3.

#### B. Continuous Class-F<sup>-1</sup> Mode Theory

Achieving very high performance in PAs requires specific fundamental and harmonic impedances to be presented to the transistor. For example, a narrowband class-F<sup>-1</sup> mode can be achieved by presenting second-harmonic open and third-harmonic short-circuit impedances at the I<sub>GEN</sub>-plane of the transistor [11]. Conventional high-efficiency-mode PAs, although

practical in many applications, are limited due to narrowband operation. These limitations extend to the biomedical applications discussed here, where the excitation frequency needs to be continually adjusted to track resonant frequency change due to volume and temperature variations in the sample.

Continuous-mode theory, targeted almost exclusively so far at mobile communications applications, provides a solution for achieving high-efficiency wideband operation [12]. Continuous class- $F^{-1}$  mode is an extended version of the narrowband class- $F^{-1}$  mode [13]. This mode of operation is achieved by ideally short-circuiting the third harmonic and presenting specific fundamental admittance and second-harmonic susceptance to the intrinsic plane of the transistor. This results in a second-harmonic peaking half-wave rectified sinusoidal voltage waveform and an “allowed” set of current waveforms which, starting as a square waveform, can change in phase, shape, and amplitude, but importantly retain power and efficiency performance. The voltage and current waveforms associated with the continuous- $F^{-1}$  mode can be generalized and are given as [13], [14]

$$I_{F^{-1}}(\alpha) = (i_{DC} - i_1 \cos \alpha + i_3 \cos 3\alpha) \quad (1)$$

$$V_{F^{-1}}(\alpha) = 1 + \frac{2}{\sqrt{2}} \cos \alpha + \frac{1}{2} \cos 2\alpha \quad (2)$$

$$I_{CF^{-1}}(\alpha) = (i_{DC} - i_1 \cos \alpha + i_3 \cos 3\alpha)(1 - \xi \sin \alpha). \quad (3)$$

Equations (1) and (2) define the standard class- $F^{-1}$  squared current waveform and second-harmonic peaking half wave rectified sinusoidal voltage waveform respectively. In this inverted continuous mode, the current waveform is allowed to vary, and this is represented by (3), where the variable  $\xi$  is introduced, and is allowed to vary between  $-1$  and  $1$ . In the load admittance environment, this is achieved, provided that fundamental and second-harmonic loads remain anti-phased as shown, for example, in Fig. 4(a), where the black circles show the allowed fundamental load admittance and the blue squares show the corresponding second-harmonic susceptances.

Therefore, by using (1)–(3), it can be seen how the loads can be distributed over, in this case, the admittance plane, and used to target wideband design space. Note that, although in this application the load presented to the transistor will be varying due to sample volume variation as well as frequency variation, the concept still holds. The current and voltage waveforms for this continuous class- $F^{-1}$  mode PA are shown in Fig. 4(b).

### C. Transistor Characterization Using Active Harmonic Load-Pull and Waveform Engineering

Active harmonic load-pull is an advanced technique used for rapid transistor characterization, and, when coupled with waveform engineering techniques, is particularly useful in determining and emulating the optimum fundamental and harmonic impedances for specific modes or classes of transistor operation [15].

As a starting point, a 10-W GaN power transistor (NXP CLF1G0060-10) was selected for this experiment. To apply load-pull measurement and waveform engineering techniques

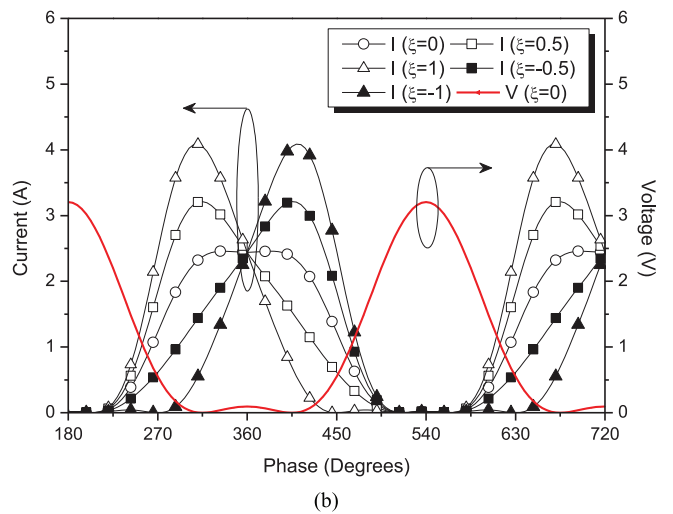
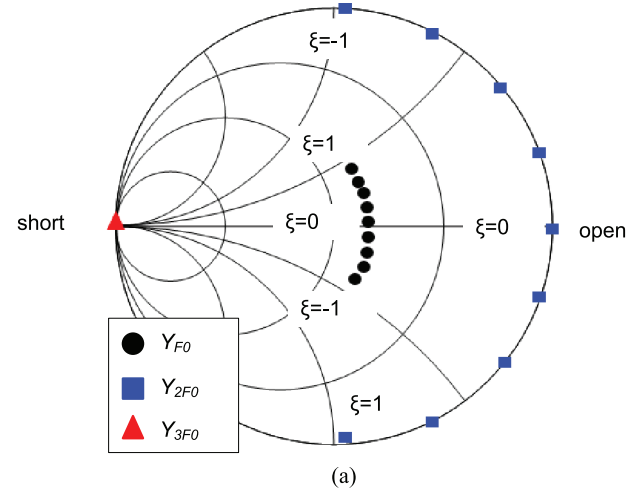


Fig. 4. (a) Ideal contours of continuous class- $F^{-1}$  loading conditions. (b) Ideal contours class- $F^{-1}$  resulting waveform combinations.

[15], the transistor was first de-embedded to its intrinsic (real)  $I_{GEN}$ -plane, where the output waveforms are free from the effects of any package-related impedance transformation and can be viewed accurately in relation to the transistors boundary conditions established by the dc  $I$ - $V$  characteristics. The package parasitic network required for de-embedding was provided by the manufacturer. Simulating these package parasitic networks within *Keysight ADS* provided  $S$ -parameter data that was then used with *Mesuro* commercially available measurement and load-pull software to modify the calibrated reference plane from that of the package plane (established using a TRL calibration) to the intrinsic plane within each transistor, for subsequent measurement. The photograph of the test setup used in this measurement exercise can be seen in [13, Fig. 8].

A design frequency 2.45 GHz was selected and the transistor was biased in approximate class-A ( $V_{ds} = 28$  V;  $V_{gs} = -1.2$  V,  $I_{ds} = 400$  mA).

As the continuous class- $F^{-1}$  is based on overdriven class-A, this was the starting point for the characterization. Load-pull measurement techniques were then applied at the intrinsic plane of the transistor and approximate class- $F^{-1}$  voltage and current waveforms were engineered, as shown in Fig. 5.



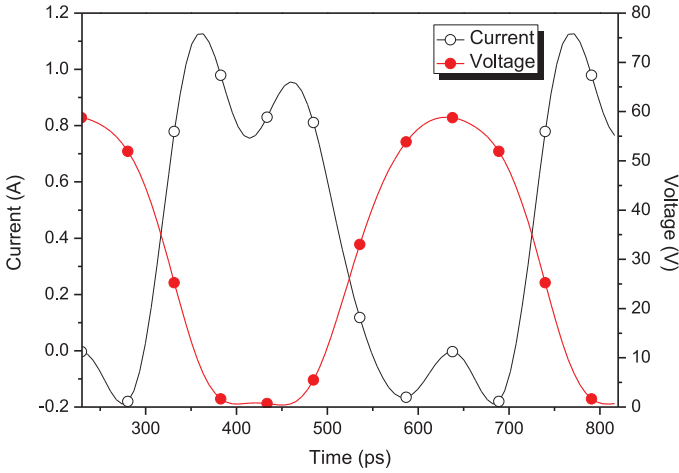


Fig. 5. Measured class- $F^{-1}$  waveforms at  $I_{GEN}$ -plane of a 10-W GaN power transistor at  $f = 2.45$  GHz.

In this state, the measured 10-W GaN transistor delivered 84% drain efficiency at 10.12-W output power at 2.45 GHz. Using this as a starting point, and by applying (1)–(3), the narrowband measured  $F^{-1}$  current waveforms can be extended to continuous class- $F^{-1}$  over a specified range of  $\xi$   $[-1$  to  $1]$ . Although the measured waveforms shown in Fig. 5 are not perfect, “textbook” class- $F^{-1}$ , this represented a good starting point. To extend the class- $F^{-1}$  mode to continuous class- $F^{-1}$ , the next step was to consider the natural cavity resonator impedance environment and to design a simplified output matching network capable of arranging the identified cavity loads at the intrinsic plane of the transistor, and hence to achieve optimal performance over operational range.

#### D. Integrated Continuous- $F^{-1}$ PA Design Approach

As already discussed, a correct impedance matching network is a critical requirement for realizing high-efficiency PA modes. Low-pass filtering methods using multistage low-pass networks discussed in [16] and [17] or stepped-impedance transformer approaches discussed in [18] can be used to present the required loading conditions for high-efficiency PA modes designed in 50- $\Omega$  environments.

To be able to present the required continuous class- $F^{-1}$  loading conditions over the cavity bandwidth, simple series transmission lines were used in conjunction with the transistor’s package parasitics. Line dimensions were adjusted until the fundamental and second-harmonic loads were as close as possible to their optimum locations. The simulated results, depicted in Fig. 6, clearly show that by using simple ideal series transmission lines, it is possible to transfer the discrete cavity loads (on the right) to the optimum points of the transistor (on the left), as identified in earlier load-pull measurements, allowing an integrated continuous mode PA structure to be realized. It is important to highlight here that a perfect third harmonic short circuit cannot be realized using this simple technique. Although it may be possible to add an extra stub to short circuit the third harmonic, this would introduce additional loss and periphery to the proposed compact design. To investigate the impact of this, the load at third-harmonic frequency was systematically

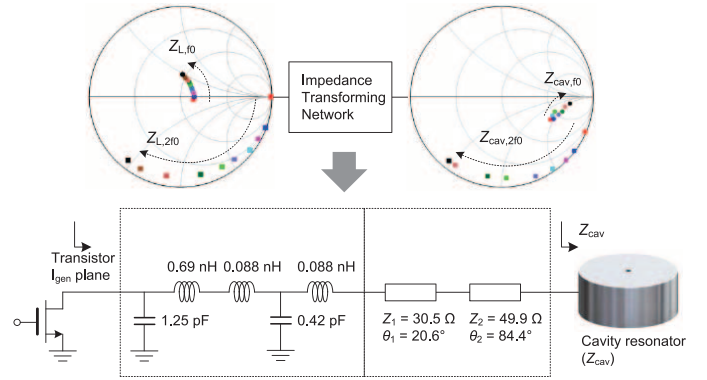


Fig. 6. Continuous- $F^{-1}$  harmonic matching network topology using microstrip lines on RT/Duroid 5880 ( $\epsilon_r = 2.2$ ,  $H = 0.5$  mm,  $\tan \delta = 0.0004$ ) substrate. The Smith chart on the right shows measured cavity loads, and the Smith chart on the left shows transformed continuous-mode impedances at the device current generator plane.

varied around the outside of the Smith chart and only 1%–2% variation in PA drain efficiency was observed.

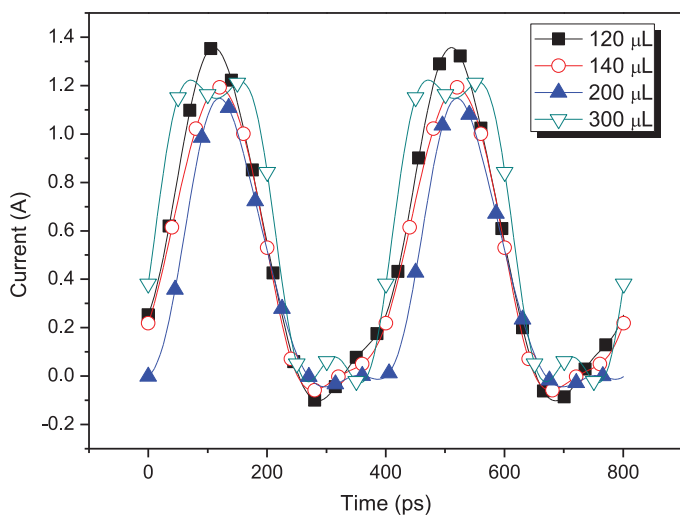
The design was completed by converting the ideal transmission lines to microstrip lines using RT duroid-5880 substrate ( $\epsilon_r = 2.2$ ,  $H = 0.5$  mm,  $\tan \delta = 0.0004$ ) and the physical lengths and widths of the lines were calculated. The final integrated PA design was simulated using ADS software, and continuous class- $F^{-1}$  waveforms were obtained at the de-embedded  $I_{GEN}$ -plane as shown in Fig. 7.

Simulations using the NXP CLFIG0060-10 transistor package model clearly show the expected second-harmonic peaking half rectified sinusoidal voltage waveform (only varying slightly) and set of phase-shifted current waveforms (with a central square waveform), clearly showing the continuous class- $F^{-1}$  mode of operation. Note that, importantly, this set of high-power, high-efficiency continuous-mode waveforms correspond to actual changes in the load impedance environment due to varying sample volume conditions.

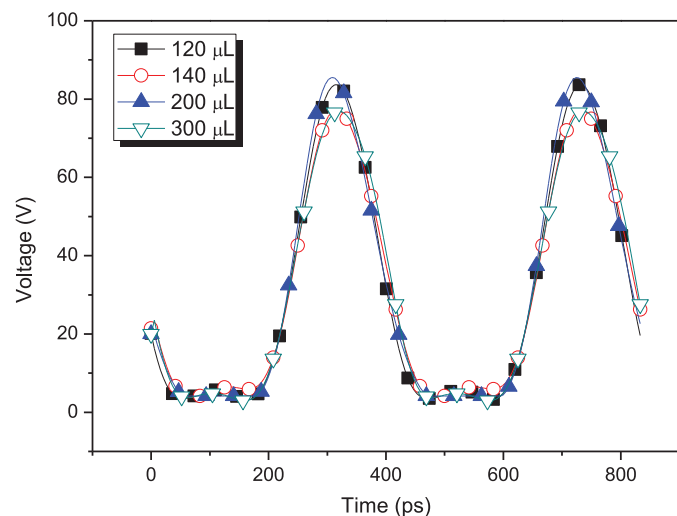
The efficient RF power delivery into the cavity is another important objective. Thus, after engineering a continuous class- $F^{-1}$  mode of the PA under discrete loading conditions, it was important to be able to monitor the reflected power between the cavity and the matched PA. The effectiveness of the complete matching network, including the embedded package parasitic network was confirmed through simulation, by presenting a range of measured cavity loads at the output (right-hand side) of the final matching network between 2.3 and 2.6 GHz (operational bandwidth of the cavity). Simple S-parameter sweeps were conducted for each selected load. Simulation results utilizing the measured cavity data clearly show that for discrete loading conditions, the return loss, from the perspective of the device’s  $I_{GEN}$ -plane, can be maintained below 10 dB for the majority of samples, which, is deemed acceptable as it will result in 90% of the power being delivered to the cavity, as shown in Fig. 8.

#### E. Directional Coupler Design and Calibration

An integrated directional coupler was used to measure the degree of mismatch between the source and load and specifically



(a)



(b)

Fig. 7. Simulated continuous class- $F^{-1}$  waveforms obtained at the Intrinsic Plane of 10-W GaN transistor using (NXP CLF1G0060-10) transistor package model. (a) Current waveforms. (b) Voltage waveforms.

the amount or reflected power. Typically, PA performance can be determined using conventional, standard  $50\text{-}\Omega$  directional couplers, where the power reflected can be measured along with power delivered to the load.

Within the available timeframe for this research, it proved difficult to properly design a coupled-line directional coupler for large-signal measurements [18]. In light of this, the integrated directional coupler was designed within the EDA (Keysight Technologies ADS) environment using a CAD-based empirical approach. The coupler was evaluated using a 2.5D EM simulation tool (Momentum) under different loading conditions, and the resulting coupler behavior was used as a simple calibration to correct the actual measurement data and obtain an approximation of the power delivered to the cavity. It is acknowledged that this was not the optimal approach, but was the only option possible with the timeframe of the project.

As research progresses and capability improves, the authors' intention is to verify the coupler behavior in a number of ways:

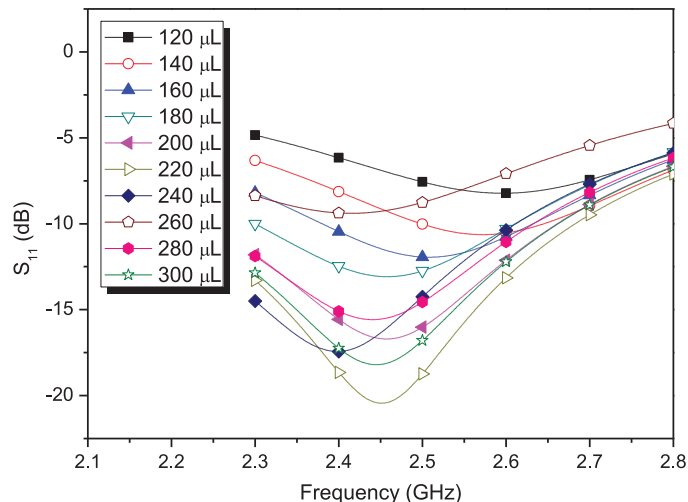


Fig. 8.  $S_{11}$  of the integrated  $TM_{010}$ -mode circular cavity resonator for varying sample volumes.

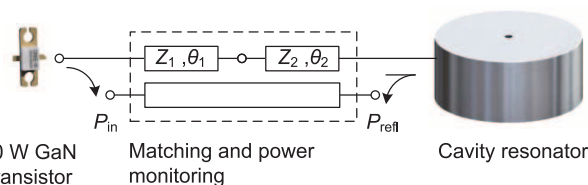


Fig. 9. Output matching network and incident and reflected power monitoring by quarter-wave directional coupler.

using a specialist thermal imaging camera to look inside the cavity and measure directly the power delivered into the sample and to implement a one-port calibration together with active load-pull techniques. Fig. 9 shows the method used in monitoring incident and reflected power from the cavity by using a directional coupler.

### III. FABRICATION AND MEASUREMENTS

After designing the integrated microwave heating arrangement, the simplified continuous class- $F^{-1}$  PA design was fabricated, and the printed circuit board (PCB) board was manufactured, as shown in Fig. 10. Compared with the conventional continuous inverted-F PAs, the board dimensions in this case were found to be  $40 \times 45 \text{ mm}^2$  with only series matching lines which, to the best of the authors' knowledge, are the record reduced dimensions.

To begin the measurements, the PA was biased to its class-A ( $V_{ds} = 28 \text{ V}$ ;  $V_{gs} = -1.2 \text{ V}$ ,  $I_{ds} = 400 \text{ mA}$ ) and the cavity was initially loaded with  $200\text{-}\mu\text{L}$  water. The loop antenna housed inside the cavity was adjusted and coupled into its magnetic field. The method described in Section II-A was implemented by systematically preparing ten water samples for separate measurements. On the other hand, to generate RF power for heating the samples, the CW carrier (at  $2.435 \text{ GHz}$ ) was generated by MXG signal generator and boosted up to  $26 \text{ dBm}$  by a driver PA. The integrated PA was driven up to its  $1 \text{ dB}$  compression point ( $26 \text{ dBm}$ ) and the RF signal analyzer (EXA-9010A) was attached to the coupling port of

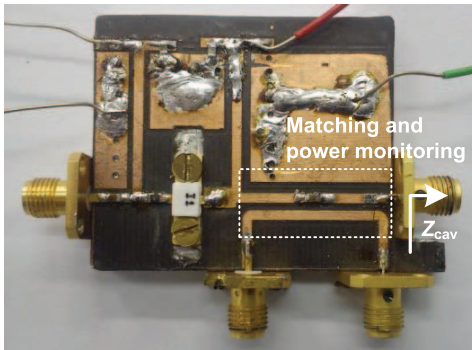


Fig. 10. Fabricated continuous  $F^{-1}$  PA with series lines and built-in directional coupler.

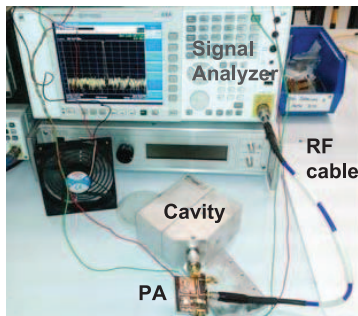
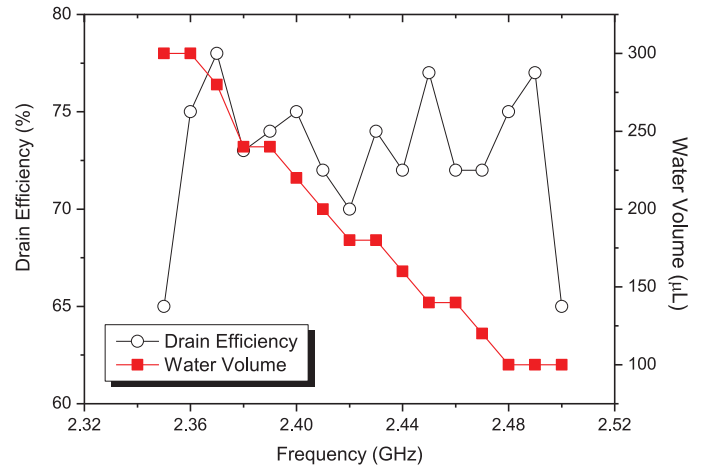


Fig. 11. Photograph of the measurement setup showing a PA connected to resonant cavity and spectrum analyzer via directional coupler.

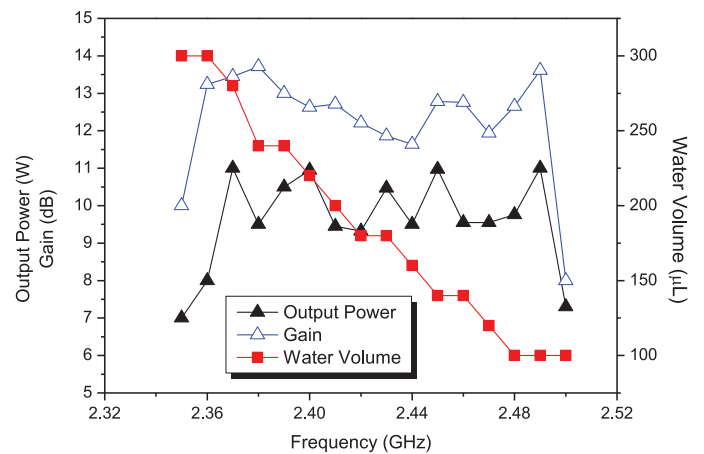
the embedded and fully calibrated directional coupler as shown in Fig. 11.

Predefined loading conditions and systematic variation in water volume and frequency resulted in specific, arranged impedances (continuous class- $F^{-1}$ ) at the current generator plane of the 10-W GaN transistor, and the expected (shown through simulation) continuous-mode RF performance was measured over the operational bandwidth of the cavity and is shown in Fig. 12(a) and (b). One case for the measured PA performance has been shown in Fig. 11, where the cavity was loaded with 200  $\mu\text{L}$  and the coupled signal was sensed by the calibrated signal analyzer at 2.435 GHz. Similarly, different water samples were loaded inside the cavity resonator and the corresponding dc power consumption and the RF power generations were measured through a systematic selection of water samples and frequency.

The integrated structure maintained a measured average efficiency over the operational bandwidth (2.37–2.49 GHz) above 70% while delivering a minimum continuous output power of 9.5 W with an average 10.2 W delivered for all water volumes. Although the measured results depicted in Fig. 12 show an excellent continuous RF performance of the fully integrated PA structure, the small variations in the output power and the drain efficiency show the fabrication tolerance and the small variable coupling loss of the embedded directional coupler (accounted in EM simulation), which is a design characteristic of the coupled-line directional couplers in a high-power measurement environment.



(a)



(b)

Fig. 12. Measured performance of the integrated PA over change in sample volume. (a) Frequency response of drain efficiency. (b) Frequency response of output power and gain.

#### IV. CONCLUSION

In this paper, a highly efficient and broadband solid-state microwave heating structure has been presented. The integrated microwave heating apparatus has been targeted for portable and field-deployable diagnostic healthcare applications. The proposed apparatus is capable of accommodating (heating) multiple water samples of different volumes while guaranteeing high-efficiency operation of the PA and minimizing the reflections from the cavity resonator.

The technique adopted in this paper follows the direct integration approach where the circular cavity is directly attached to the 10-W GaN power transistor and the continuous class- $F^{-1}$  mode of operation has been achieved by utilizing the water-dependent cavity loads together with the simple series delay line and the built-in package network of the transistor. Under continuous-inverse-F loading conditions, the apparatus demonstrated a high RF performance (average drain efficiency > 70%) over the functional bandwidth of the cavity (2.37–2.49 GHz). The integrated design also contains an integrated directional coupler that offers a continuous performance monitoring mechanism and adds to the further compactness of the system. Due to its small size, flexibility, and light weight, this apparatus can be installed and operated bedside for sample diagnosis.

## ACKNOWLEDGMENT

The authors would like to thank and acknowledge the support of K. Werner and R. Jon Marlow, NXP Semiconductors, Manchester, U.K., for providing the 10-W GaN power transistor used in this experiment. The authors would also like to thank F. Shkal for helping in simulations. In addition, the authors acknowledge the support of Ser Cymru National Research Network NRN075.

## REFERENCES

- [1] H. D. Trefna and M. Persson, "Antenna array design for brain monitoring," in *Proc. IEEE Int. Microw. Symp. Antennas Propag. Soc.*, San Diego, CA, USA, Jul. 2008, pp. 1–4.
- [2] M. A. Khorshidi, T. Mckelvey, M. Persson, and H. D. Trefna, "Classification of microwave scattering data based on a subspace distance with application to bleeding stroke," in *Proc. 3rd IEEE Int. Workshop on Computational Advances in Multi-Sensor Adaptive Process.*, Aruba, Dutch Antilles, Dec. 2009, pp. 301–304.
- [3] H. D. Trefna, A. Imtiaz, H. Lui, and M. Persson, "Evolution of an UWB antenna for hyperthermia array applicator," in *Proc. 6th Eur. Conf. Antennas Propag.*, Prague, Czech Republic, Mar. 2012, pp. 1046–1048.
- [4] Y. Abed, A. Devin-Regli, and C. Bollet, "Efficient discrimination of mycobacterium tuberculosis strains by 16S-23S spacer region based random amplified polymorphic DNA analysis," *J. Microbiol. Biotechnol.*, vol. 5, no. 33, pp. 1418–1420, Nov. 1995.
- [5] A. Imtiaz, Z. A. Mokhti, J. Cuenca, and J. Lees, "An integrated inverse-F power amplifier design approach for heating applications in a microwave resonant cavity," in *Proc. Asia-Pacific Microw. Conf.*, Sendai, Japan, Nov. 2014, pp. 756–758.
- [6] A. Imtiaz, J. Hartley, H. Choi, and J. Lees, "A high power high efficiency integrated solid-state microwave heating structure for portable diagnostic healthcare applications," in *Proc. IEEE MTT-S Int. Microw. Workshop Series for Biomedical and Healthcare Applications*, London, U.K., Dec. 2014, pp. 1–3.
- [7] K. Chen and D. Peroulis, "Design of broadband high-efficiency power amplifier using in-band class-F<sup>-1</sup>/F mode transferring technique," in *IEEE MTT-S Int. Microw. Symp. Digest*, Montreal, QC, Canada, Jun. 2012, pp. 17–22.
- [8] K. Chen and D. Peroulis, "Design of broadband highly efficient harmonic-tuned power amplifier using in-band continuous class (F<sup>-1</sup>/F) mode transferring," *IEEE Trans. Microw. Theory Techn.*, vol. 60, no. 12, pp. 4107–4116, Dec. 2012.
- [9] T. Hermann, G. R. Olbrich, and P. Russer, "A novel microwave-based inspection system for continuously streaming materials using a cavity resonator," in *Proc. 38th Eur. Microw. Conf.*, Amsterdam, The Netherlands, Oct. 2008, pp. 901–904.
- [10] J. Jow, M. C. Hawley, M. C. Finzel, and Asmussen Jr., "Microwave heating and dielectric diagnosis technique in a single-mode resonant cavity," *Rev. Scientific Instrum.*, vol. 60, no. 1, pp. 96–103, Jan. 1989.
- [11] A. Grebennikov, "Load network design techniques for class-F and inv.F PAs," *High Frequency Electron.*, pp. 58–76, May 2011.
- [12] V. Carubba, A. L. Clarke, M. Akmal, J. Lees, J. Benedikt, P. J. Tasker, and S. C. Cripps, "The continuous class-F mode power amplifier," in *Proc. Eur. Microw. Integr. Circuits Conf.*, Paris, France, Sep. 2010, pp. 432–435.
- [13] V. Carubba, A. L. Clarke, M. Akmal, J. Lees, J. Benedikt, S. C. Cripps, and P. J. Tasker, "The continuous inverse-F mode power amplifier with resistive second harmonic impedance," *IEEE Trans. Microw. Theory Techn.*, vol. 60, no. 6, pp. 1928–1936, Jun. 2010.
- [14] P. J. Tasker, "Practical waveform engineering," *IEEE Microw. Mag.*, vol. 10, no. 7, pp. 65–76, Dec. 2009.
- [15] N. Tuffy, L. Guan, A. Zhu, and T. J. Brazil, "A simplified broadband design methodology for linearized high-Efficiency continuous class-F power amplifiers," *IEEE Trans. Microw. Theory Techn.*, vol. 60, no. 6, pp. 1952–1963, Jun. 2012.
- [16] J. Moon, J. Son, J. Lees, and B. Kim, "A multimode/multiband envelope tracking transmitter with broadband saturated power amplifier," *IEEE Trans. Microw. Theory Techn.*, vol. 59, no. 12, pp. 3463–3473, Dec. 2011.
- [17] D. M. Pozar, *Microwave Engineering*, 3rd ed. New York, NY, USA: Wiley, 2005.
- [18] J. A. G. Malherbe, *Microwave Transmission Line Filters*. Dedham, MA, USA: Artech, 1979.



**Azeem Imtiaz** (M'15) received the first B.S (Hons) degree in physics from the University of Punjab, Lahore, Pakistan, in 2004, the B.S (Hons) degree in electronic engineering from International Islamic University Islamabad, Pakistan, in 2008, and the M.Sc. degree in electronic/telecommunication engineering from the University of Gavle, Gayle, Sweden, in 2011. He is currently working toward the Ph.D. degree at Cardiff University, Cardiff, U.K.

He is currently with the Centre for High Frequency Engineering, School of Engineering, Cardiff University, Cardiff, U.K. His research activities include the development of a high-power, high-efficiency, compact, broadband, and field-deployable solid-state microwave heating structure suitable for portable diagnostic healthcare applications.



**Jonathan Lees** received the M.Sc. and Ph.D. degrees from Cardiff University, Cardiff, U.K., in 2001 and 2006, respectively.

He is currently a Lecturer within Cardiff University's Centre for High Frequency Engineering (CHFE), Cardiff, U.K. At the start of his career, his research focus was the nonlinear characterization and optimization of high-efficiency power amplifiers and the study of device nonlinearity and linearization using modulated time-domain and envelope-domain techniques. His work in this area culminated in the first published GaN Doherty amplifier. He previously worked for ten years developing optical and GPS-based positional tracking solutions with QinetiQ (U.K.). In recent years, he has applied his microwave expertise to medical applications, including the design of highly integrated microwave power amplifiers for diagnostic applications and the generation and use of high-power pulsed microwave energy for the detection of *C. difficile*. He is actively involved in the supervision of over ten Ph.D. students, as well as two research associates. He has published over 90 refereed publications including 18 journal papers, and his current research projects include integrating high-efficiency amplifiers with antennas (Ser Cymru NRN), development and realization of novel broadband high-efficiency power amplifiers (EU-Eureka/Celtic – OperaNET), and the generation and use of high-power pulsed microwave energy for the detection of *C. difficile* (Cardiff Partnership Fund/School of Pharmacy at Cardiff).



**Heungjae Choi** (S'06–M'11) received the B.S., M.S., and Ph.D. degrees in electronic engineering from Chonbuk National University, Jeonju, Korea, in 2004, 2006, and 2011, respectively.

From 2006 to 2011, he served an alternative military service as a Specialty Researcher while working towards his Ph.D. degree. He is currently a Post-Doctoral Research Associate with the Centre for High Frequency Engineering, Cardiff University, Cardiff, U.K. From 2011 to 2012, he has worked on the development of ultrafast active harmonic load-pull system development as a collaboration with National Instruments and had two successful live demonstrations at the 2012 European Microwave Week, Amsterdam, The Netherlands, and the 2013 IEEE Radio and Wireless Week, Austin, TX, USA. Since 2013, he has been working on the development of a noninvasive blood glucose monitoring sensor system and clinical trials funded by the Wellcome Trust. He has authored or coauthored over 50 papers in peer-reviewed journals and conference proceedings. His research interests include microwave circuits, especially high-efficiency power amplifiers and linearizers, and their application to material characterization and biomedical engineering.

Dr. Choi has served as a reviewer for the IEEE MICROWAVE AND WIRELESS COMPONENTS LETTERS, the IEEE TRANSACTIONS ON CIRCUITS AND SYSTEMS II—EXPRESS BRIEFS, *Progress in Electromagnetics Research*, the *IET Microwaves, Antennas & Propagation*, and the *International Journal of Antennas and Propagation*. He was the recipient of the Outstanding Achievement Award at Student High Efficiency Power Amplifier Design Competition at the 2008 IEEE Microwave Theory and Techniques Society (MTT-S) International Microwave Symposium (IMS) and the 2010 Samsung Human Tech Thesis Prize Awards.





**Lovleen Tina Joshi** received B.Sc. and Ph.D. degrees in microbiology from Cardiff University, Cardiff, U.K., in 2008 and 2012, respectively.

Her final-year project while at Cardiff University focused on the effects of oxidative stress on insertion sequences in *Burkholderia cenocepacia*. In the summer of 2008, she undertook a Society for Applied Microbiology (SfAM) summer studentship at Cardiff School of Pharmacy and Pharmaceutical sciences, focusing on biological

aspects of the Gram positive bacterium *C. difficile*. Following this studentship, she started her doctoral studies with Prof. Les Baillie in October 2008 on the “Pathogenicity and a bedside real time detection assay for *Clostridium difficile* in the faeces of hospitalized patients.” As part of her doctoral work, she spent three months in Baltimore, MD, USA, developing and testing the resulting rapid pathogen detector technologies at the Institute of Fluorescence with Dr. Chris Geddes (UMBC). She is currently a Post-Doctoral Researcher with Cardiff University School of Pharmacy and Pharmaceutical Sciences to further develop and enhance the rapid detection technologies for *C. difficile* and *Bacillus anthracis*.